29 Mar 2001, 4:00 pm - 6:00 pm

Effect of K_0 on Liquefaction Strength of Silty Sand

Shun-ichi Sawada
OYO Corporation, Japan

Ryouichi Sakuraba
OYO Corporation, Japan

Naoki Ohmukai
OYO Corporation, Japan

Takeko Mikami
OYO Corporation, Japan

EFFECT OF K_0 ON LIQUEFACTION STRENGTH OF SILTY SAND

Sawada Shun-ichi
OYO Corporation
Technical Center
Omiya, Saitama,
330-8632, Japan

Sakuraba Ryouichi
OYO Corporation
Tokyo Branch
Bunkyo, Tokyo,
112-0012,Japan

Ohmukai Naoki
OYO Corporation
Core-Laboratory
Omiya, Saitama,
330-0038, Japan

Mikami Takeko
OYO Corporation
Core-Laboratory
Omiya, Saitama,
330-0038, Japan

ABSTRACT

Authors measured K_0–value in-situ using Self-boring lateral load tester (SBLLT) and Flat-diratometer (DMT). After that, a series of cyclic undrained torsional shear tests under the plane strain condition on anisotropically consolidated condition (K_0–condition) has been performed using undisturbed tube sampling to investigate the relation between the liquefaction strength of isotropically consolidated condition ($Rl_{isotropic}$) and K_0–condition (Rl_{K0}). The result of these laboratory tests shows that the liquefaction strength defined as 7.5% shear strain in double amplitude of undisturbed silty sand is generally agreement between triaxial and torsional test with isotropically and anisotropically consolidation. However, the cyclic behavior up to liquefaction strength defined as 7.5% shear strain in double amplitude was a greatly difference in stress condition.

KEYWORDS

Liquefaction, K_0 consolidation, sandy soil, torsional shear, pressuremeter test, in-situ test, laboratory test.

INTRODUCTION

It is still fresh in our memories that a lot of structures were greatly damaged by 1995 Hyogoken-Nambu Earthquake. The major caused of these damages was liquefaction. Liquefaction phenomena have been widely observed in seismic active regions. Although investigations on liquefaction have been concentrated mainly on clean sand deposits, some liquefaction phenomena due to recent earthquakes were found in reclaimed deposits that were composed of sands containing considerable amount of fines. It has been very important to estimate accurate liquefaction potential because of predicting earthquake liquefaction damages. Generally, we obtain the detailed liquefaction strength (Rl_{20}) using the cyclic undrained triaxial tests with isotropically consolidation. However it is important to consider the estimation of coefficient of lateral earth pressure at rest (the following, K_0–value) in-situ because the ground is known for anisotropy condition which is characterized by stress conditions in horizontal and vertical direction. This paper describes the behavior of silty sand in the cyclic undrained strength by cyclic torsional shear tests and cyclic undrained triaxial tests. The cyclic behavior is discussed in connection with the behavior on anisotropically consolidated condition. Laboratory tests used to be adopted to evaluate the liquefaction strength after undisturbed tube sampling.

GROUND CONDITIONS IN SITE

Undisturbed tube sampling undergone is located in the reclaimed land near the Tokyo Bay. The soil profile and N-values by the standard penetration test (SPT) are shown in Fig.1. Problematic soil in the sampling field is the part of hydraulic fills that were constructed by dredging. The fills are mainly consisted of fine sand with shell fragments and interbedded with clayey-silt thin layer. And also, N-values of SPT in the fills are less than 10 blows that show relatively loose sandy soils. These fills develop from the surface to about 10m in depth above natural loose sand layer underlying normal marine clay to 30m in depth. The main grain size distributions of the fills are shown in Fig.2. According to both N-values and grain size distribution of fills, it is estimated that the fills have a great potential of liquefaction by earthquake.

SITE INVESTIGATION IN FIELD

In-site tests including the flat-diratometer (DMT) and the self-boring lateral load tester (SBLLT) carried out. DMT was performed using 1989-version equipment developed by Marchetti (1980;See Fig.3). The vertical depth increment used

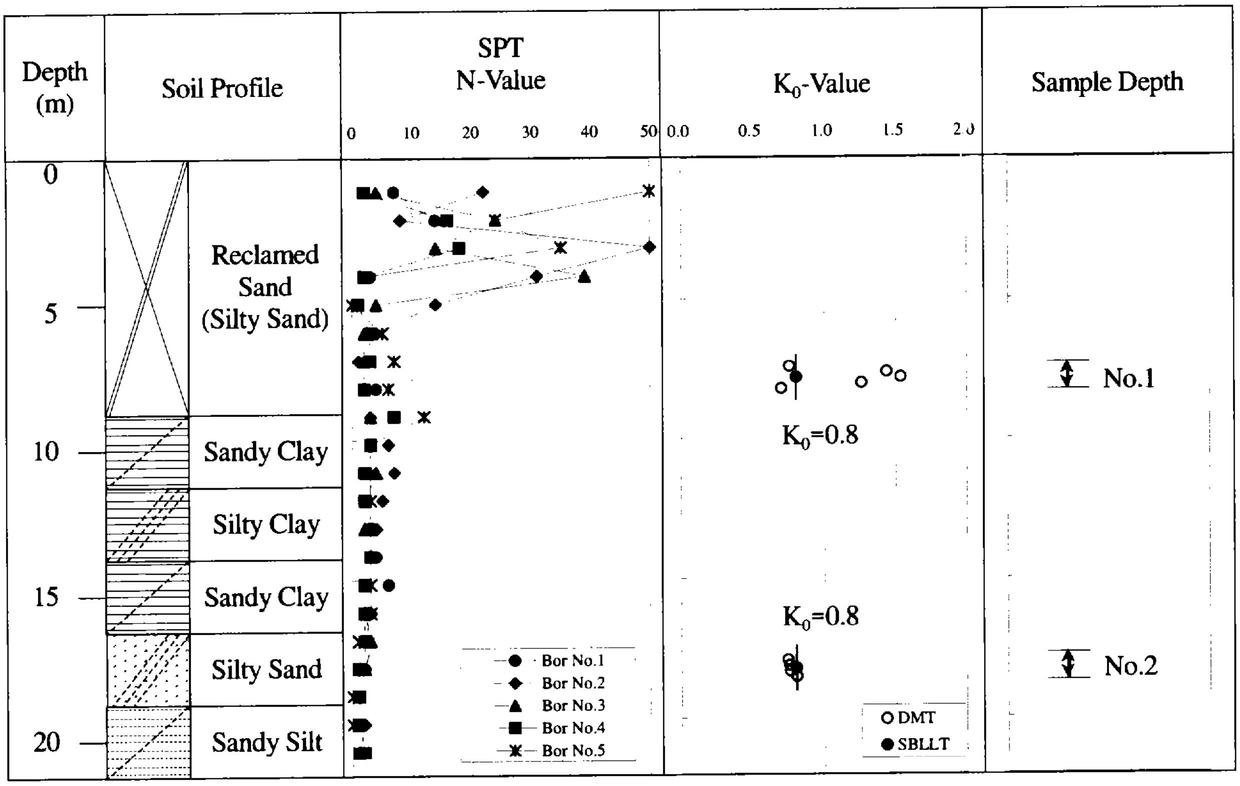

Fig.1 Soil profiles in the sampling site

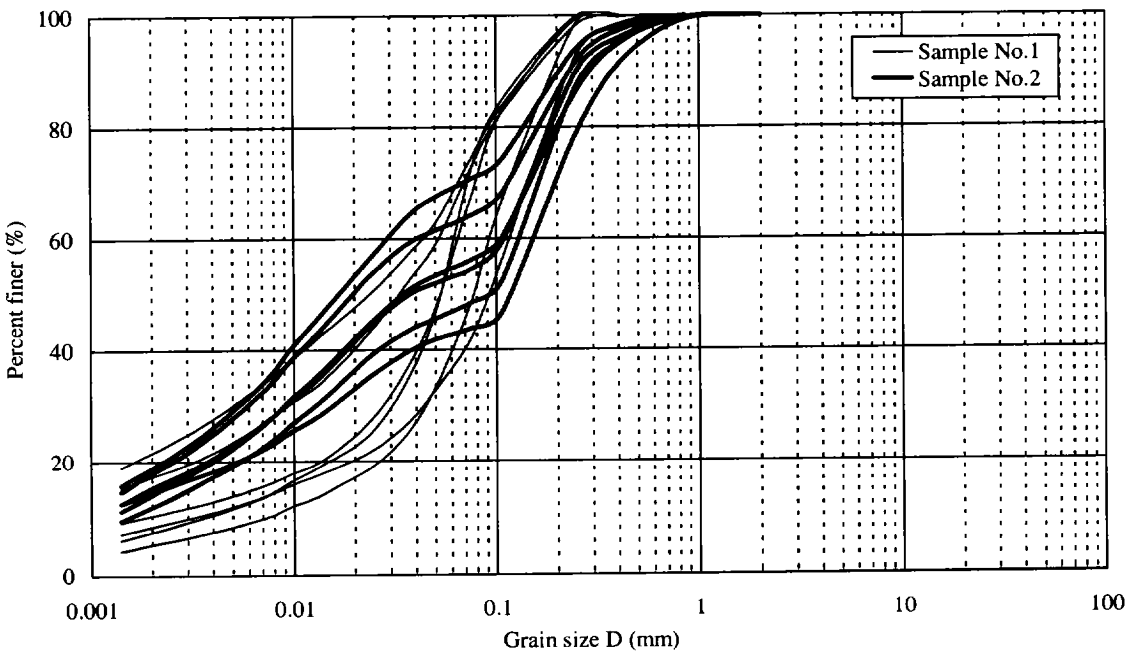

Fig.2 Main grain size distributions of reclaimed sandy soil in the sampling layer

in DMT sounding is 20cm by advancing the blade using static push of boring rod. The SBLLT probe developed by Clark et al (1989; See Fig. 4) was used in the site. The probe is 73.6mm in diameter 450mm long, i. e., the ratio of length to diameter is 6.1. Three displacement transducers installed in the probe located at 120° around the circumference, to measure the probe expansion with sensitivity of 0.001mm and a pressure transducer with maximum pressure of 5 MPa to measure inner pressure. The expansion of the membrane was stress controlled and continues to over 10% of radial strain. Before 5% of radial strain is over, several unload/reload cycles of different cavity strain amplitudes were included. Generally, the reclaimed ground is known to be not necessarily uniform. A few investigation data in complicated soil such condition may lead judgment to mistake. In order to confirm the validity of judgement according to the result of SBLLT, results obtained from DMT were supplied. The variations of K_0–value with depth on sampling ground were shown in Fig.1. The ground condition of sampling depth is not necessary uniform, although the roughly average of K_0–value is 0.8 at the both sampling depths.

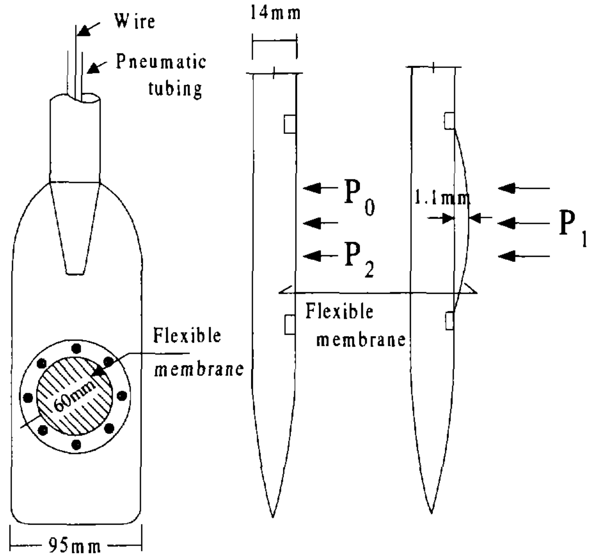

Fig.3 Schematic diagram of the Flat-diratometer blade

LABORATORY TEST PROSEDURES

Table-1 shows the comparison between in-situ and laboratory tests of stress condition. Before shaking by an earthquake, an element of saturated soil under level ground has undergone a long-term consolidation process under K_0 conditions. This soil element is subjected undrained to a sequence of shear stress cyclic during an earthquake as illustrated in Table-1(a). The ordinary test for liquefaction strength is elucidated from observation of the behavior of a soil sample undergoing cyclic stress application in the laboratory triaxial test apparatus. This loading procedure creates stress condition on plane of 45° through the sample which is the same as those produce on the horizontal plane in the ground during earthquakes. The stress conditions at each stage of loading in the cyclic undrained triaxial test are illustrated in Table-1(b). When the axial stress σ_d is applied undrained, the shear stress induced on the 45° degree plane is σ_d /2. And given that those soil samples are clean sand without fine contents, the normal stress σ_d /2 is also induced on this plane but this purely compressive component of σ_d /2 which is mostly transmitted to pore water without inducing any change in the existing effect confining stress σ_r. Therefore the normal stress acting on the 45° plane can be disregarded. When simulating the level ground condition, the cyclic torsional shear stress must be applied while inhibiting lateral deformation as illustrated Table-1(c). This type of test will be referred to as the anisotropically consolidated conditioned torsion test. The schematic diagram of cyclic torsional shear test and cyclic undrained triaxial test as shown in Fig.5.

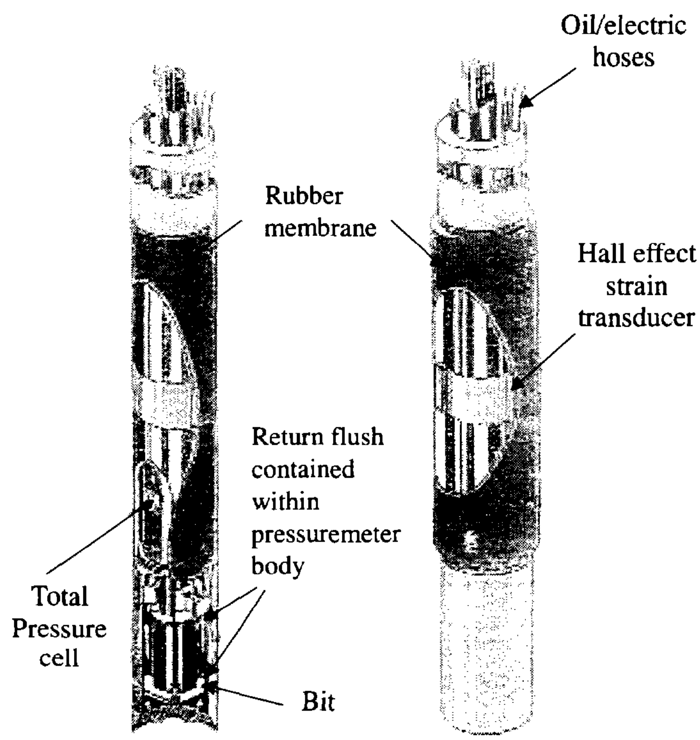

Fig.4 Schematic diagram of Self-boring pressuremeter probe

Table-1 Comparison between in-situ and laboratory tests with stress condition

Type \ Item	Stress condition	Mohr's stress circle	Consolidation condition & Deformation
(a) In-situ	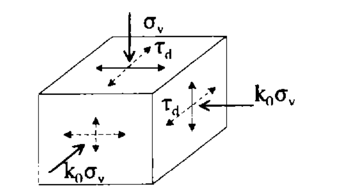	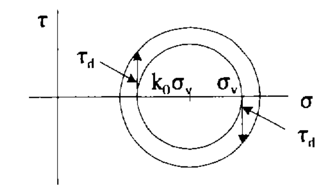	Anisotropically consolidated condition (Ko-condition) & Simple shear deformation
(b) Cyclic triaxial test	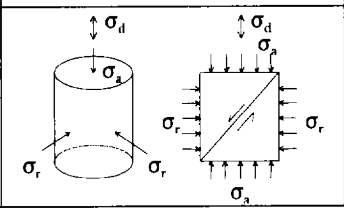	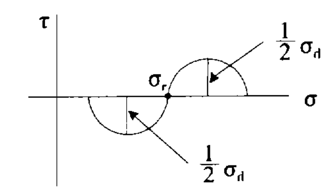	Isotropically consolidated condition & Axisymmetrically deformation
(c) Cyclic torsional shear test	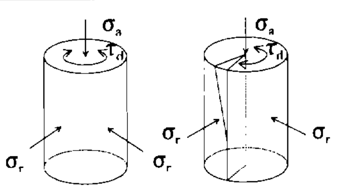	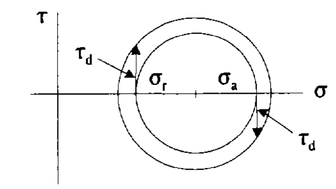	Isotropically or Anisotropically consolidated condition & Simple shear deformation

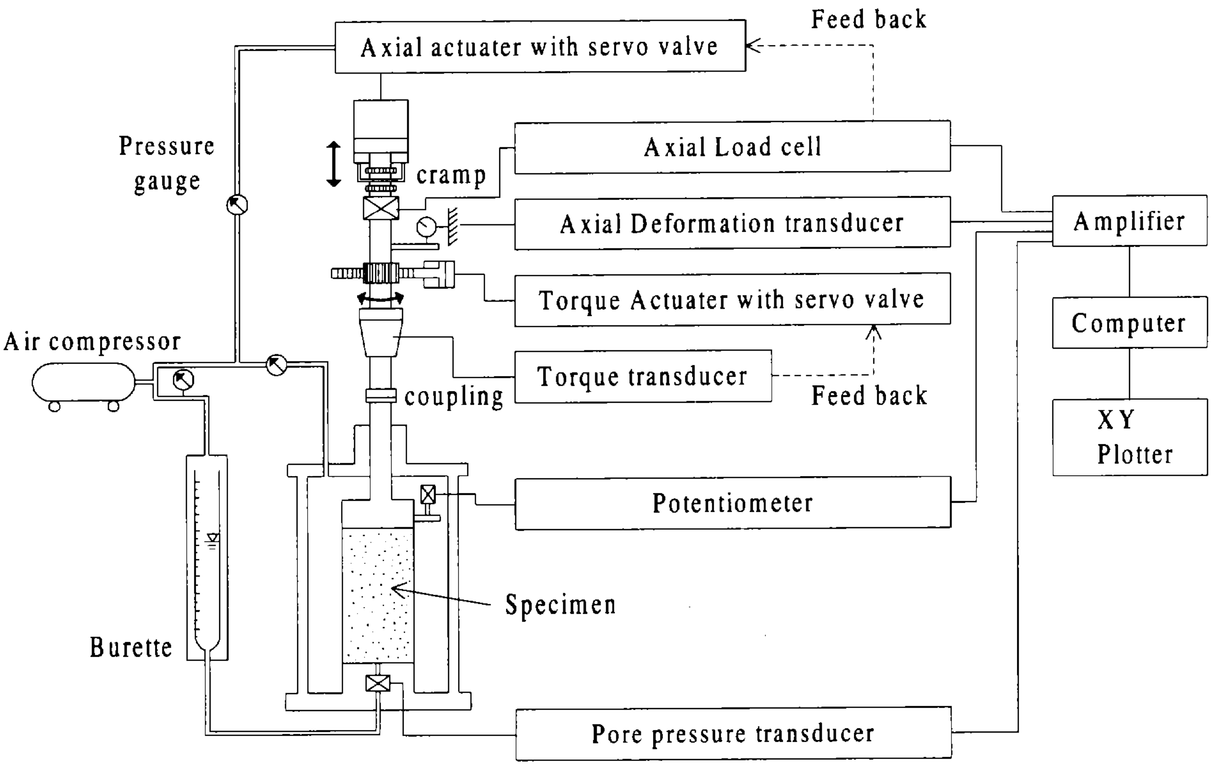

Fig.5 Apparatus of cyclic torsional shear test and cyclic undrained triaxial test

Table-2 indicates the stress condition of laboratory test procedures and the physical properties of samples used in the tests. There are two series of soil samples. The both series of soil samples were carried out laboratory tests under two dynamic shear stress;τ_d and three stress conditions as followed.
(1)Cyclic torsional shear condition with isotropically consolidation (Laterally free).
(2)Cyclic torsional shear condition with K_0 consolidation (Lateral constraint).
(3)Cyclic undrained triaxial condition.
The initial mean effective confining pressures of all specimens were equal through the relation,

$$\sigma_{m0}' = \frac{\sigma_a' + 2\,\sigma_r'}{3} = \frac{(1+2\,k_0)\,\sigma_a'}{3}$$

Undrained cyclic loading tests were performed using sine wave loads with a frequency of 0.1 Hz, after the stress histories of isotropically or anisotropically consolidation were applied to the specimen. In all tests, the specimens were saturated in excess of a B-value of 0.95 by circulating carbon dioxide, CO_2, and deaired water.

CYCLIC BEHAVIOR OF VARIOUS STRESS CONDITIONS

The typical variations of initial stress condition (The series No. 1-A), shear strain and excess pore pressure with the number of cycles are shown in Fig. 6(a) and Fig. 6(b), respectively. Fig. 7 shows a relationship between shear stress and shear strain. The effective stress paths for same test condition are presented in Fig. 8. Fig. 9 shows a relationship between dynamic maximum shear stress and dynamic maximum shear strain, in which the ordinate indicates an equivalent dynamic maximum shear stress τ_{maxd} and dynamic maximum shear strain γ_{maxd} defined by

$$\tau_{maxd} = \sqrt{((\sigma_a' - \sigma_r')^2/4 + \tau_\theta^2)}$$

$$\gamma_{maxd} = \sqrt{(1+\nu)^2 \varepsilon_a^2 + \gamma_\theta^2}$$

where σ_a' :Axial effective stress
σ_r' :Radial effective stress
ε_a :Axial strain on cyclic triaxial test
τ_θ :Torsional stress on cyclic torsional shear test
γ_θ :Torsional strain on cyclic torsional shear test
ν :Poisson's ratio = 0.5.

Table-2 The stress condition of laboratory test procedures and the physical properties of samples

Sample No. (Depth of sampling)	1 (G.L.-6.99 ~ -7.79m)						2 (G.L.-17.42 ~ -18.19m)					
Specimen No.	1-A-1	1-A-2	1-A-3	1-B-1	1-B-2	1-B-3	2-A-1	2-A-2	2-A-3	2-B-1	2-B-2	2-B-3
Loading Type	Torsional	Torsional	Triaxial	Torsional	Torsional	Triaxial	Torsional	Torsional	Triaxial	Torsional	Torsional	Triaxial
Axial cramp	free	fixed	-	free	fixed	-	free	fixed	-	free	fixed	-
K_0-value	1.0	0.8	1.0	1.0	0.8	1.0	1.0	0.8	1.0	1.0	0.8	1.0
σ'_a (kN/m^2)	58	67	58	58	67	58	58	67	58	58	67	58
σ'_r (kN/m^2)	58	54	58	58	54	58	58	54	58	58	54	58
Density of soil particle (g/cm^3)	2.752	2.746	2.742	2.736	2.740	2.727	2.791	2.788	2.777	2.786	2.799	2.791
Water content (%)	38.55	42.95	31.47	46.78	51.65	40.61	65.23	60.37	52.35	62.14	83.26	93.96
Wet density (g/cm^3)	1.794	1.780	1.885	1.738	1.691	1.781	1.618	1.645	1.697	1.629	1.522	1.470
Gravel fraction (%)	0	0	0	0	0	0	0	0	0	0	0	0
Sand fraction (%)	51	28	58	27	26	32	44	45	56	51	36	29
Silt fraction (%)	41	61	31	49	43	55	33	32	24	30	35	41
Clay fraction (%)	8	11	11	24	31	13	23	23	20	19	29	30

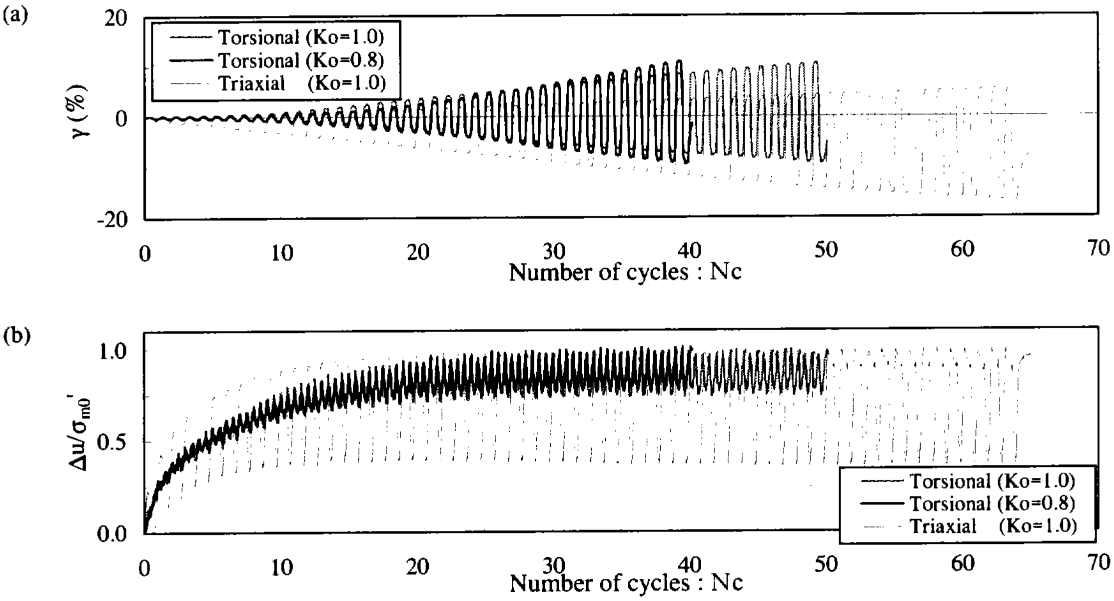

Fig.6 Shear strain and excess pore pressure with the number of cycles

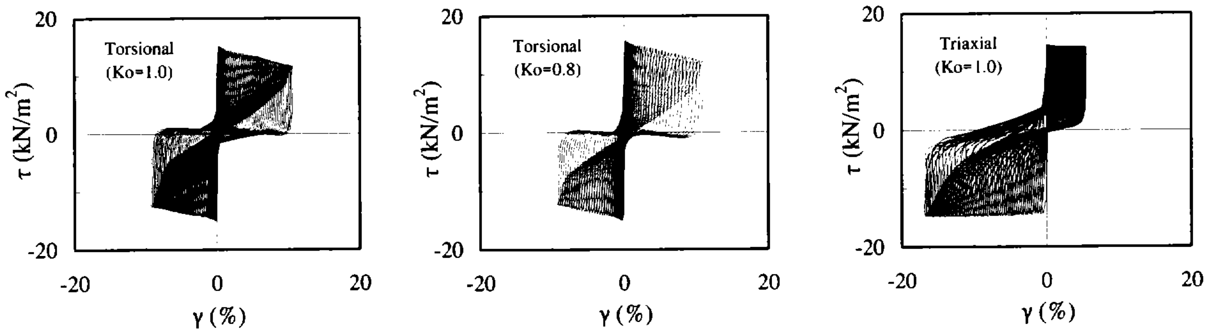

Fig.7 Relationship between shear stress and shear strain

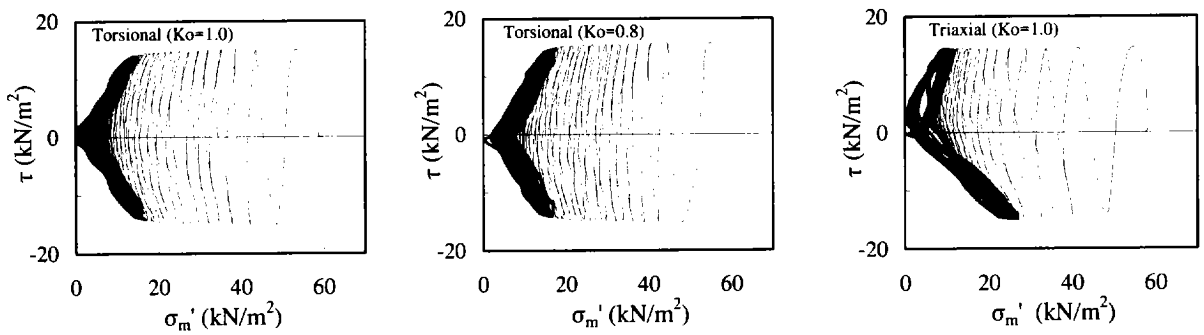

Fig.8 Effective stress path

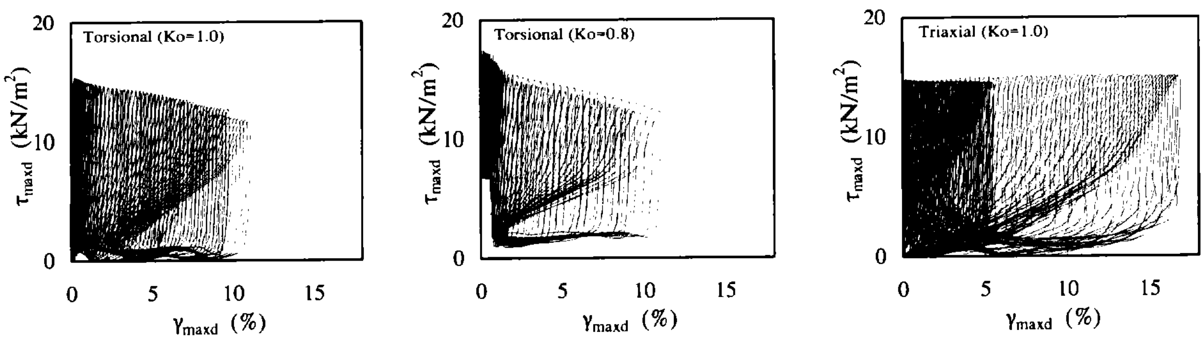

Fig.9 Relationship between dynamic maximum shear stress and dynamic maximum shear strain

In case of cyclic torsional shear tests, the behavior of shear strain is symmetrical. However, in case of cyclic undrained triaxial test, most of the shear strain occurred in extension which is characteristic of silty sand. The reason why this tendency is the effective confining pressure is decrease, when the cyclic axial stress direction is extension. Therefore, the shear strain increases to extension direction. In the case of cyclic torsional shear test with anisotropically consolidated results, the pore pressure measured at the bottom of the specimen through the pedestal did not develop up to the initial confining stress. And it is observed that the amplitude of excess pore pressure in cyclic torsional shear tests is larger than the cyclic undrained triaxial test. The effective stress path moved towards the failure envelopes during cyclic loading and finally traced a steady loop which reach the failure envelopes for both the compression and extension sides. Both figures the relationship between shear stress and shear strain and the relationship between dynamic maximum shear stress and dynamic maximum shear strain clearly indicate that the tendency of shear strain developed is unsymmetrical behavior between compression and extension sides.

DEVEROPMENT OF SHEAR STRAIN AND EXCESS PORE PRESSURE RATIO

The development of shear strain and excess pore pressure in cyclic torsional shear tests for intact specimens were investigated for the evaluation of the development of an excess pore water pressure in situ soils during earthquake motions. Excess pore water pressure ratio $\Delta u/\sigma'_{m0}$, at the number of cyclic loading Nc, in cyclic torsional test was defined as the value of excess pore water pressure ratio just after the cyclic loading at Nc was completed. Fig. 10 shows the relationships between shear strain γ and Nc/(Nc for 7.5% shear strain in double amplitude). And Fig. 11 shows the relationships between $\Delta u/\sigma'_{m0}$ and Nc/(Nc for γ_{DA}=7.5%). σ'_{m0} is the initial effective confining pressure and (Nc for γ_{DA}=7.5%) is the number of cyclic loading at which the double amplitude of shear strain (γ_{DA}) become 7.5%. The stress condition appears to affect the behavior of excess pore pressure and shear strain up to liquefaction strength of silty sand. In case of cyclic undrained triaxial test, it is observed that the shear strain tends to increase with increasing normalized number of cycles like a straight line. On the other hand, in case of cyclic torsional test, this relation likes an exponential.

CYCLIC SHEAR STRENGTH

The effect of K_0 consolidation and cyclic stress condition on cyclic shear strength is expressed by the cyclic stress ratio τ/σ'_{m0} which a specified double amplitude shear strain. Fig. 11 present the relationship between cyclic stress ratio and number of cycles to induce 1.5%, 3.0%, 7.5% and 10% shear strain in double amplitude respective at various stress conditions. It is observed that the cyclic shear strength curve of the large shear strain like 7.5% which is liquefaction strength get small difference between cyclic torsional test and cyclic undrained triaxial test. On the other hand, the difference of the cyclic shear strength at small shear strain like 1.5% becomes large. In other words, it is clearly shows that the difference between the number of cycles to 1.5% shear strain in double amplitude and 7.5% tends to increase with increasing cyclic stress ratio.
It is important to note the difference those cyclic shear strengths at small shear strain, because in order to evaluate the properties of the soils under cyclic loading, numerical analysts determined in these cyclic shear strengths.

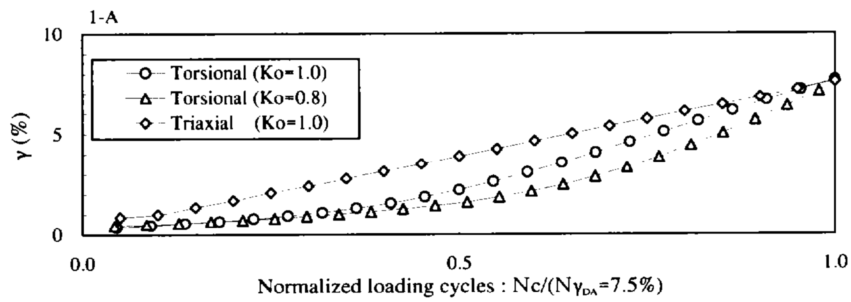

Fig.10 Relationships between shear strain and normalized loading cycles

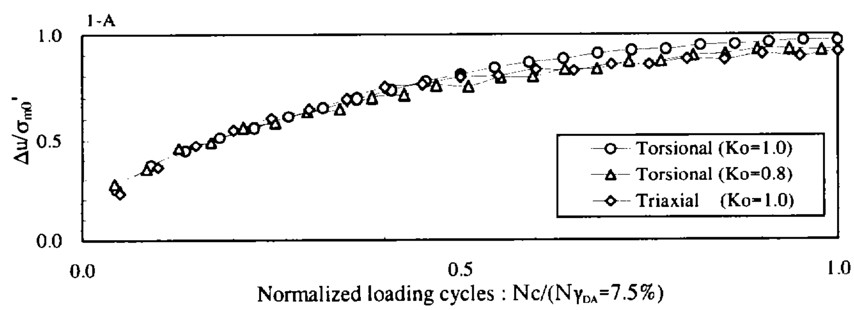

Fig.11 Relationships between excess pore pressure ratio and normalized loading cycles

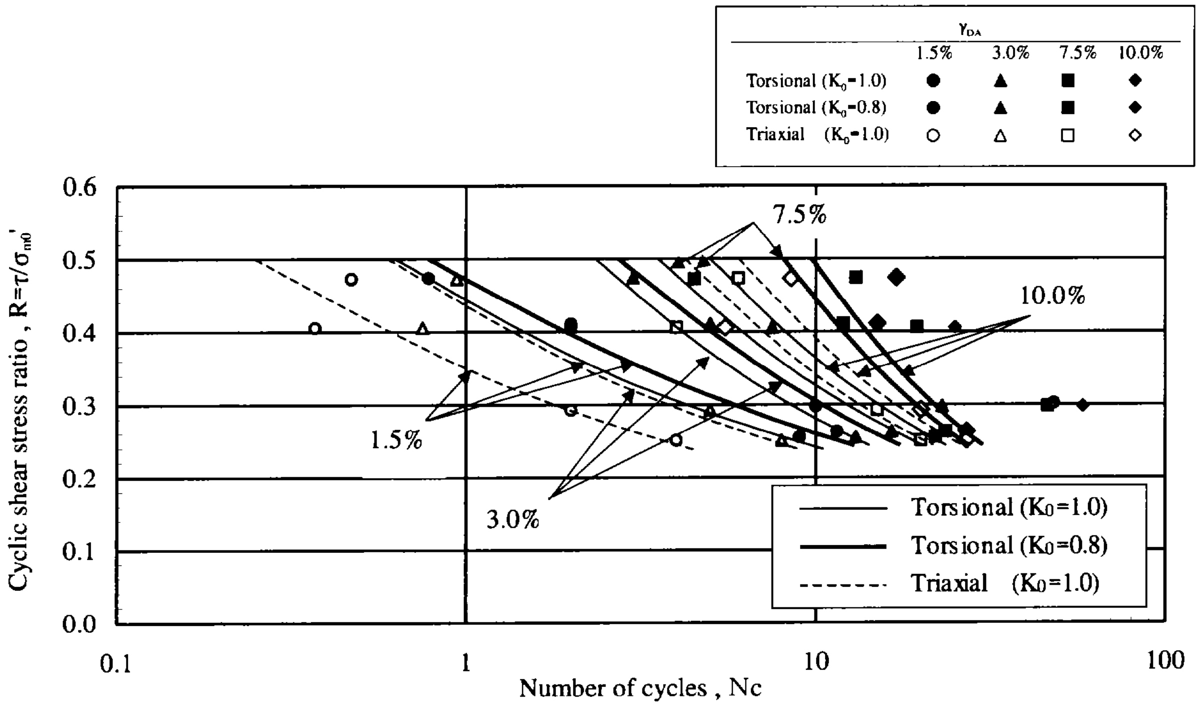

Fig.12 Relationships between cyclic shear stress ratio and the number of cycles to reach γ_{DA}=1.5% , 3.0% , 7.5% and 10.0%

CONCLUSIONS

Several series of laboratory tests on undisturbed sample were performed to examine the effect of K_0 consolidation and stress conditions on cyclic shear strength of silty sand.The following conclusions were reached based on the laboratory tests.

(1)The result of these laboratory tests shows that the liquefaction strength defined as 7.5% shear strain in double amplitude of undisturbed silty sand is generally agreement between triaxial and torsional test with isotropically and anisotropically consolidation.

(2)The stress condition appears to affect the behavior of excess pore pressure and shear strain up to liquefaction strength of silty sand. In particular, the behavior of the cyclic undrained triaxial tests is different stress condition between in-situ and laboratory.

(3)It was noteworthy that the minimum cyclic shear strength was observed at cyclic undrained triaxial test that is ordinary used in small shear strain up to 7.5% in double amplitude. The main reason for this behavior is that the effective confining pressure is decrease, when the cyclic axial stress direction is extension.

(4)It was observed that the shear strain on anisotropically consolidated specimen (K_0–condition) up to liquefaction strength was smaller than isotropically consolidation.

REFERENCES

Marchetti,S [1980]. "In situ tests by flat dilatometer, Journal of the Geotechnical Engineering Division", ASCE, Vol.106, No.GT3, pp.299-321.

Clark B.G. and A.Smith [1992]. "Self-boring Pressuremeter Test in Weak Rocks", Construction and Building Materials, Vol. 6, No.2, pp.91-95.

Sawada, S. & N. Sugawara [1995]. "Evaluation of densification of loose sand by SBP and DMT" 4th International Symposium of the Pressuremeter and its New Avenues, pp101-107.

Watanabe, N., H.Hamada, J.Koseki, Y.Koga & A.Takahashi [1991]. "Permanent Deformation Characteristics of Saturated Sands under Static and Cyclic shear Stress Loading" 26th Japan National Conference on Soil Mechanics and Foundation Engineering, pp.731-734, July 1991 (in Japanese).

Iwasaki, T. & F.Tatsuok [1997]. "Effect of Grain Size and Grading on Dynamic Shear Moduli of Sands" Soil and Foundations, Vol.17, No.3 pp.19-35, 1977.

Ishihara, K. [1993]. "Liquefaction and flow failure during earthquake" 33rd Rankine lecture, Geotechnique 43, No.3 pp.351-415.

Kuwano, J., B.Sapkota, H.Hashizume & K.Tanaka [1993]. "Liquefaction characteristics of sand containing fines" Tsuchi-to-Kiso, JSSMFE 41, No.7, pp.23-28 (in Japanese).